Magne, J., Bucciarelli-Ducci, C., Dahl, J. S., Gimelli, A., Haugaa, K. H., Miller, O., ... Popescu, B. A. (2018). EuroEcho-imaging 2017: highlights. *European Heart Journal - Cardiovascular Imaging*, *19*(5), 482-489. https://doi.org/10.1093/ehjci/jey037

Abstract

The annual meeting of the European Association of Cardiovascular Imaging, EuroEcho-Imaging, was held in Lisbon, Portugal, in December 2017. In the present paper, we present a summary of the 'Highlights' session.

Key words: heart failure, heart valve disease, new technologies, congenital heart disease, nuclear cardiology, cardiac computed tomography, cardiac magnetic resonance

The twenty-first annual scientific meeting of the European Association of Cardiovascular Imaging (EACVI), EuroEcho-Imaging 2017, was held in December in Lisbon, Portugal. The main themes were “Imaging in heart failure” and “interventional imaging”.

The meeting was a great success with the highest number of participants ever with 3 973 delegates and over 1 414 abstracts and clinical cases submitted.

Overall, 128 abstracts and clinical cases were accepted as oral presentation, 86 moderated posters and 985 posters were presented. Of note, the preferred topics regarding abstracts submission were “Assessment of morphology and function”, “Heart valves”, “Tissue Doppler and speckle tracking”, “Cardiomyopathies” and “Systemic diseases and other conditions”.

The ‘Highlights’ session wrapped up the event with a summary of the most relevant abstracts presented throughout the congress on the last day of the meeting. A short report of this session is presented below.

Heart Failure

Reis et al.[1] investigated gender-correlated differences in a population with hypertrophic cardiomyopathy (HCM) in a Portuguese multicentre study. They included 567 HCM patients from 12 hospitals and followed them for 8.0±6.1 years. While women with HCM were older and more symptomatic than males, there were no differences in progression to chronic heart failure, medical treatment, implantation of intra cardiac defibrillator (ICD), arrhythmias, HCM-related mortality, risk of sudden death, stroke and all-cause mortality. Therefore, unlike previous studies, in this study, female gender was not associated with a worse prognosis

The value of the CHA2DS2-VASc risk score and modified Fabry-specific score were studied by Hu et al.[2] aiming to predict new-onset or recurrent stroke/transient ischemic attack (TIA) in patients with Fabry disease without atrial fibrillation. They included 159 patients with Fabry disease. During 5 years of follow up, 10% had new onset or recurrent stroke. Risk factors were prior stroke, angiokeratoma, creatinine ≥1 mg/dl, left ventricular posterior wall diameter >14mm and global longitudinal strain worse than -13.5%. The Fabry-specific score based on these risk factors was superior to classic CHA_2DS_2-VASc risk score on predicting new-onset or recurrent stroke/TIA and could potentially help decisions on anticoagulation therapy in patients with Fabry.

Stampfli et al.[3] studied patients with left ventricular non-compaction cardiomyopathy (LVNC) with focus on right ventricular morphology and function. By CMR, they compared 20 LVNC patients with 20 controls and found more trabeculation in the right ventricle (RV) by CMR in patients compared to healthy. Also amount of RV and LV trabeculation correlated closely in

LVNC patients. These findings suggest that LVNC is a biventricular disease, morphologically affecting both LV and RV to a similar extent.

Lie et al.[4] presented echocardiographic parameters to predict life-threatening ventricular arrhythmia in patients with arrhythmogenic cardiomyopathy (AC). In a prospective cohort of 167 AC patients without previous arrhythmias, 15% had life threatening arrhythmias during 4.2 years of follow up. The LV mechanical dispersion and RV global strain were the best predictors for ventricular arrhythmias. Presence of both risk markers included a 50% risk of ventricular arrhythmias within 2 years and could be helpful in decisions on primary prevention ICD implantation (Figure 1).

In a population of 316 patients with heart transplant of which 17 patients suffered from severe rejection, Cordeiro et al.[5] found that those with severe humoral rejection showed a worsening in global longitudinal and circumferential strain before rejection. In contrast, patients with cellular rejection did not. Therefore, global strain assessment by echocardiography may allow an early detection of a developing humoral graft rejection.

Dobutamine stress echocardiography was performed by Tereshina et al.[6] in 27 patients with chemotherapy-induced LV dysfunction and they followed the patients for 1 year. Absence of contractile reserve by dobutamine stress echocardiography was associated with a higher risk of further progression of ventricular dysfunction.

Clerc et al.[7] performed a direct comparison of single-photon emission computed tomography (SPECT), coronary artery calcium score (CACS), coronary CT angiography (CCTA), combined SPECT+CACS and hybrid SPECT/CCTA for long-term prediction of major cardiac events. They followed 380 patients for 6.3 years. Framingham risk score and SPECT were inferior risk markers compared to the other tested modalities. The CCTA and CACS score had highest predictive values for major cardiac events.

New technologies

Regional left ventricular (LV) myocardial work can be assessed non-invasively by pressure-strain loops (PSL) using speckle-tracking echocardiography (STE). Galli et al.[8] used PSL to measure constructive and wasted work (CW and WW) in 97 left bundle branch block (LBBB) patients undergoing cardiac resynchronization therapy (CRT). At univariate analyses, they showed that CW and WW, as well as other standard echocardiographic parameters were predictors of CRT response. In multivariable analysis, the addition of CW and WW led to a

significant increase in the model prediction, suggesting that PSL analysis might be a promising tool for assessing CRT candidates.

In an experimental study, Aalen et al.[9] found that moderate elevation of afterload in 11 patients with isolated LBBB caused marked reduction in septal work. If confirmed, these preliminary findings could have implications for blood pressure evaluation and treatment goals in CRT candidates.

Klæboe et al.[10] used 3D echocardiography (3DE) and STE to compare LV geometry and function in 20 patients with hypertrophic cardiomyopathy (HCM) genotype positive with mild phenotype (LV wall thickness 12-16 mm) versus 30 competitive athletes with similar LV mass and ejection fraction. Despite having similar values of global longitudinal strain, the HCM patients had smaller 3DE LV volumes and more pronounced mechanical dispersion (MD), a cut-off value of MD $\geq$ 44ms optimally discriminating patients from athletes.

Rodríguez-Zanella et al.[11] assessed the value of LV MD to predict the risk of severe arrhythmias and sudden death in 96 patients with structural heart disease followed for 44±20 months. Using a recently described limit of normality of MD $\geq$56ms, the authors found that that MD is a powerful independent predictor of major arrhythmic events, and allows additional prognostic stratification in patients with LV ejection fraction (EF) >35% (Figure 2).

Mirea O et al.[12] compared the accuracy of STE algorithms from 8 different vendors to identify scarred myocardium in 58 patients with previous myocardial infarction. They found that post-systolic strain index enables to discriminate among segments with transmural, non-transmural and no scar, however there were significant differences in the accuracy of different algorithms, suggesting need of further standardization from EACVI/ASE/Industry TaskForce to achieve interchangeable results among different vendors.

The RV EF assessed by 3DE has been demonstrated to be a significant predictor of all-cause mortality in an unselected cohort of 297 patients with various cardiovascular diseases follow-up during 3.7±1.1 year by Prevedello et al.[13] The RV EF was superior to conventional RV functional parameters for predicting outcome.

Using 3DE in 18 patients before and after mitral valve surgery, Lakatos et al.[14] demonstrated a marked decrease in RV longitudinal shortening after surgery, with a compensatory increase in RV radial function ("bellows" effect) to preserve RV stroke volume and EF.

In patients with pulmonary hypertension, Palumbo et al.[15] found that interventricular septum curvature quantified by 3DE had a strong positive correlation with pulmonary arterial

pressure. These studies highlight the potential of 3DE to provide a better outcome stratification and understanding of RV function.

Heart valve diseases

Contemporary data on outcome after isolated tricuspid valve surgery (ITVS), was provided based on a large nationwide population including all patients undergoing this procedure in France from 2013-2014[16]. Among 241 patients undergoing ITVS, in-hospital mortality was 10%, the combined end-point of death, need for dialysis and ECMO occurred in 19% and there was a mean hospitalization duration of 26 days. Congestive heart failure at presentation was the sole factor associated with in-hospital mortality, suggesting that patients should be referred for ITVS before the development of RV failure.

Fries et al.[17] presented 10 years follow-up data based on a previous described cohort of 58 patients with severe aortic stenosis (AS) who underwent a myocardial biopsy during aortic valve replacement (AVR) and no signs of coronary disease. Patients with severe fibrosis did not improve symptoms and 74% died after 10 years, underlining the impact of fibrosis on outcome in AS. Future studies should be conducted to demonstrate if AVR before the development of fibrosis may improve outcome.

The clinical importance of pressure recovery in patients with AS was studied in 111 patients with asymptomatic severe AS and LVEF>50%[18]. One fourth of patients had a pressure recovery ≥20mmHg. Patients likely to experience pressure recovery, e.g. aorta diameter<30mm and ratio of effective orifice area to aorta diameter>0.2cm, had a better prognosis in terms of AVR and all-cause mortality. These findings need to be corroborated in future studies.

Paravalvular leakage (PVL) is a strong marker of outcome in patients with AS undergoing TAVR. Among 147 patients undergoing TAVR Sanchis et al.[19] demonstrated that patients with moderate-severe PVL had larger LV septal-bulge height compared to those with mild PVL (3.6±1.2 vs. 5.2±1.6mm, p<0.001), despite demonstrating similar septal wall-thickness. This was particularly prevalent among patients treated with supra-annular self-expanding prosthesis.

The accuracy of CT aortic valve calcium (AVC) score in determining calcium concentration in patients with severe AS, was studied in 69 explanted valves[20]. The valves were CT-scanned ex-vivo and later dissolved into an acid solution in order to calculate calcium concentration. A modest correlation (r^2=0.62) was demonstrated between AVC and valvular calcium

concentration, suggesting that AVC is more dependent of the total calcium amount rather than valvular calcium concentration.

The recently proposed algorithms by the American Society of Echocardiography for grading aortic regurgitation (AR) and mitral regurgitation (MR) were tested in two separate studies[21-22]. Forty-five patients with AR underwent cardiac magnetic resonance (CMR) study and a transthoracic echocardiography (TTE), simultaneously. The algorithm demonstrated a sensitivity of 95% and a specificity of 63% for differentiating severe from non-severe AR. In 16% of patients AR grading was not possible due to feasibility problems. Similarly, 48 patients with MR, predominantly as a consequence of valve prolapse, underwent CMR and a TTE. The algorithm showed a specificity of 86% and a specificity of 80% in differentiating between severe and non-severe MR, although it particularly was good rolling in severe MR. Furthermore, these studies demonstrated modest correlations between echocardiographic measures of regurgitation severity and CMR in both AR and MR, emphasizing the importance of the use of an integrative approach using both quantitative and qualitative measures when grading regurgitation severity.

The usefulness of novel software able to automatically trace the MR continuous wave-Doppler envelope and calculating the average pixel intensity (Figure 3) was studied in 112 patients with mitral valve prolapse and MR. Acquisition was feasible in 89% of patients, demonstrated excellent reproducibility, and correlated well (r=0.90) with the effective regurgitation orifice area. The authors concluded that the method was fast, easy and reproducible and may have potential advantages over current MR severity assessment methods[23].

Congenital heart disease

Adults with repaired coarctation have reduced life expectancy. Exercising such patients, Di Salvo et al.[24] showed hypertension, residual pressure gradient, an increase in LV mass and decreased global longitudinal strain.

Across the range of bicuspid aortic valve (BAV) phenotypes, Aguiar Rosa et al.[25] reported flow in proximal aorta, aortic wall shear stress (WSS) and aortic valve shear stress. The turbulent high velocity flow from a BAV generated a higher WSS, leading to aortic dilatation, with BAV morphology influencing aortopathy phenotype.

Lesniak-Sobelga et al.[26] reported on BAV during pregnancy in 96 women over a 19-year period. Fifty-six patients had AS and 40 patients had AR. During pregnancy, all patients with

mild AS remained in NYHA functional class I. LV mass and aortic pressure gradients increased significantly with gestation but decreased after delivery. Volume overload of pregnancy is well tolerated in patients with mild/moderate AR, but complications increased with AR severity, LV enlargement, impaired systolic function and/or the enlargement of ascending aorta.

Ivanac et al.[27] reported from a single centre retrospective study of repaired tetralogy of Fallot (rToF) and pregnancy. Reassuringly, there was no change in NYHA class, LV size, strain and strain rate; RV global longitudinal strain rate, RV free wall strain and strain rate, RV FAC, RV S', tricuspid regurgitation or pulmonary stenosis severity.

Van De Brauene et al.[28] examined right ventricular outflow tract to pulmonary artery (RVOT-PA) anatomy with CMR in adults with repaired rToF. RVOT-PA dimensions and volumes are related to indexed RV volumes, RV mass and severity of pulmonary regurgitation (PR). RVOT-PA volumes were divided into straight, convergent, divergent, convex or concave morphologies (Figure 4). Patients with divergent RVOT-PA type may have worse NYHA class.

In 85 patients with rToF, significant PR and RV dilatation (mean 150 mL/m^2), and > 2 CMR exams during the study period (2002-2016), Hoelscher et al.[29] reported that progression of RV dilatation is infrequent (23%) and slow and advised a conservative approach to pulmonary valve replacement.

Aortic root dilatation (ARD) is frequent in rToF and may progress over time leading to complications including AR, aortic aneurysm and dissection. In a single centre study, Grotenhuis et al.[30] studied 768 children; 77% ToF, 5% Double Outlet RV (DORV)/ToF, 18% ToF/Pulmonary Atresia (PAT). The mean age at repair was 12.1±20.9 months. The aortic root was enlarged at diagnosis and during follow-up (6.3±2.2-years). The results showed a mean AoV annulus Z-score at first post-op echo of 3.3±2.7. The mean maximum AoV diameter Z-score during follow-up was 4.3±2.7, with no significant progression of ARD during follow-up. An increase in ARD at a rate >1 Z-score unit/year was observed in <1% of patients and the mean rate of Z-score change was -0.09 Z-score unit/year. Only 3/768 patients developed moderate or severe AR and 2 required aortic surgery.

Michalek et al.[31] reported neo-AR in 53 adults during late follow up (mean 20.5 years) after the Arterial Switch Operation for Transposition of the Great Arteries. TTE was used to grade NeoAR qualitatively compared to CMR severity grade based on regurgitant fraction. Both

modalities correlate well at low grades, but TTE overestimates severity (P<0.001) at moderate-severe neo-AR.

Intracardiac blood flow, WSS and energy loss (EL) using vector flow mapping and colour Doppler was reported in normal children[32], and in children with hypertrophic cardiomyopathy (HCM) and dilated cardiomyopathy (DCM) Craft et al.[33] Vector flow derived left ventricular diastolic indices in children are heart rate dependent and associated with E/e'. In HCM/DCM, predominant EL was noted in systole for HCM, but in diastole for DCM and controls. Energy loss curves showed lower amplitudes in DCM compared to controls.

Nuclear Cardiology and Cardiac Computed Tomography

The evaluation of myocardial perfusion abnormalities for the detection of ischemia by SPECT or positron emission tomography (PET) is well established. On the contrary, CCTA is widely used for diagnosis of coronary artery disease. Oleksiak et al.[34] showed that the evaluation of myocardial ischemia is feasible also by dynamic CCTA and may add diagnostic value in patients with anatomically intermediate coronary artery stenosis. To this purpose, they enrolled a series of 17 consecutive patients with intermediate stenosis detected by CCTA. Myocardial perfusion was evaluated at baseline and after vasodilation with regadenoson and compared to similar protocol obtained by CMR. The distribution of myocardial contrast agent in dynamic CCTA, was represented as quantitative parameters for each myocardial segment: myocardial blood flow (MBF), myocardial blood volume, peak value, time to peak, perfused capillary blood volume (Figure 5). The Authors concluded that in a multivariate model, MBF and peak value predicted myocardial ischemia with better accuracy compared to individual parameters.

The CT could be used also for planning specific 3D-printing. Percutaneous left atrial appendage (LAA) occlusion has emerged as an alternative approach to medical therapy for stroke prevention in patients with atrial fibrillation. Guglielmo et al.[35] evaluate whether the sizing of the implanted occluder device, based on the sole medical image analysis, was in accordance with the sizing obtained using the 3D printing mode. The final goal was to evaluate if the mismatch between two different approaches was correlated with adverse outcome, and if 3D printing could be a valuable tool to enhance the pre-operative sizing stage. The results, even if obtaining in a series of 13 patients evaluated retrospectively, were very encouraging. As a matter of fact, the results suggested that the use of 3D printing models help

in finding the correct size of the device, potentially avoiding the negative outcome of the surgery.

The CT could also be used for identifying patients who benefit more from specific surgical treatment such as mitral valve repair. Solowjowa et al.[36] investigated the possibility to optimize the surgical procedure for LV aneurysms using an algorithm based on CT assessment. In 30 consecutive patients, the mitral valve leaflets and apparatus were characterized and measured. The Authors analysed the surgically relevant differences between posterior and anterior localization, and the mid-term results of both groups. The obtained results suggested that the CT guided strategy for surgical valve repair of LV aneurysms could allow excellent mid-term results to be achieved due to adequate volume reduction and functional improvement.

Stress myocardial perfusion SPECT is clinically used for cardiovascular risk assessment prior to kidney transplantation. Berlot et al.[37] examined the predictive value of SPECT for coronary artery disease or perioperative and long-term cardiovascular events in a series of 80 consecutive patients undergoing renal transplant. Sensitivity and specificity of SPECT in identifying significant perioperative cardiovascular risk were of 100% and 84%, respectively. Moreover, reversible ischemia emerged as an independent predictor of long-term cardiovascular events following transplant. Based on these data, SPECT should be used a useful modality for cardiovascular risk stratification and to predict long-term prognosis of patients undergoing kidney transplant.

Holcman et al.[38] compared 99mTc-HMPAO-SPECT/CT and TTE diagnostic value in 40 consecutive patients with suspected infective endocarditis. Study included 6 months follow-up, followed by outpatient visit and TTE. This study highlighted and confirmed the diagnostic value of 99mTc-HMPAO-SPECT/CT in assessing infective endocarditis suspicion. In patients with suspected infective endocarditis 99mTc-HMPAO-SPECT/CT provided higher specificity and positive predictive value than TTE.

There is limited evidence regarding the comparison of vascular inflammation between subjects with familial combined hyperlipidaemia (FCH) and heterozygous familial hypercholesterolemia (heFH). Benetos et al.[39] compared the degree of arterial inflammation as assessed by 18 F fluorodeoxyglucose PET (FDG-PET) in asymptomatic individuals with FCH and heFH (both n=14). Nondyslipidaemic individuals scheduled for FDG-PET imaging were used as control group (n=14).

Radiotracer uptake within the arterial wall was quantified as target to background ratio (TBR) along the aorta. Blood lipid profile, high sensitive C reactive protein (hs-CRP) and fibrinogen were obtained from all subjects. The obtained results indicated that FCH is associated with increased both systemic and vascular inflammation, compared to heFH.

Cardiovascular magnetic resonance

The CMR myocardial feature tracking (CMR-FT) is a novel post-processing method which is receiving increasing interest due to its accurate assessment of global circumferential (GCS), radial (GRS) and longitudinal (GLS) myocardial strain,

The prognostic role of these novel functional parameters in the context of ischemic heart disease are not well established. Eitel et al.[40] conducted a large multicentre study of patients with reperfused myocardial infarction (MI) (n=1235, 64% with ST-elevation MI, 36% with non ST-elevation MI) undergoing CMR with GLS, GRS, GCS measured by a central corelab. They demonstrated that GLS was the strongest strain parameter predicting future cardiovascular events, independently of traditional established prognostic markers. In particular, GLS provided an incremental prognostic value for all-cause mortality above LV ejection fraction and infarct size. Lange et al.[41] investigated both the mechanistic and prognostic value of CMR-FT in 152 patients with Tako-Tsubo cardiomyopathy with varying type of LV apical ballooning (apical 72%, mid-ventricular 26.7% and basal 1.3%) compared to 20 healthy control subjects and to 20 patients with Tako-Tsubo rescanned at 3-month follow up. They measured systolic torsion, diastolic recoil and dyssynchrony by the means of circumferential and radial uniformity ratio estimates. They observed that dyssychrony is a distinct feature of acute Tako-Tsubo cardiomyopathy, that it is more prominent in the apical than in the midventricular ballooning and that resolves in parallel with the systolic function. Additionally, they demonstrated that higher degree of dyssynchrony is associated with impaired rotational mechanics, and that diastolic recoil identifies a subgroup of patients at high mortality risk characterized by highly impaired rotational mechanics (Figure 6). In conclusion, whilst transient circumferential dyssynchrony is a distinct feature in the acute phase, mechanical rotational performance remains impaired and predicts adverse cardiac events. There is also limited evidence on the role of CMR-FT in the context of valvular heart disease. Gonzales-Gomez et al.[42] performed a RV volumetric and deformation analysis in 13 patients with asymptomatic severe tricuspid regurgitation compared to 10 healthy controls. Despite normal and comparable RVEF and RV volumes between the 2 groups, patients with

severe tricuspid regurgitation showed impaired longitudinal and radial RV strain values compared to control. This study suggests a promising role of RV CMR-FT as an early marker of RV systolic dysfunction before RVEF declines and volumes increase. Hwang et al.[43] used CMR-FT and CMR T1 mapping to predict LV reverse remodeling in 63 patients with severe aortic stenosis before surgical aortic valve replacement. They demonstrated that strain parameters measured by CMR-FT correlated with the amount of myocardial fibrosis (native T1 mapping and interstitial fibrosis, ECV), and that reverse remodeling significantly correlated with myocardial strain with GLS independently predicting LV mass index regression.

Finally, Gertz et al.[44] proposed an important methodological piece of work of assessing inter-vendor agreement of LV/RV myocardial feature tracking. They evaluated patients with normal and abnormal LV/RV systolic function (10 patients in each group), and images were analysed in the long-and short-axis views using 2 different software vendors. They concluded that GCS and LV GLS are the most robust parameters within and between softwares, whilst GRS and RV GLS show high inter-vendor variability but with an improved and acceptable reproducibility using each software when performing repeated analyses. Intra-vendor reproducibility was excellent for GCS, LV GLS and RV GLS, but lower for GRS.

Acknowledgment

CBD is supported by the Bristol National Institute of Health Research (NIHR) Biomedical Centre at the University Hospitals Bristol NHS Foundation Trust and the University of Bristol. The views expressed in this publication are those of the author(s) and not necessarily those of the United Kingdom NHS, the National Institute for Health Research or the Department of Health.

Figures Legend

Figure 1: Left ventricular mechanical dispersion (left mid panel) and right ventricular longitudinal strain (left lower panel) were strong predictors of ventricular arrhythmias in patients with arrhythmogenic cardiomyopathy.

Figure 2: Kaplan-Meier survival curves, showing the value of left ventricular mechanical dispersion (MD) ≥56 ms to predict survival free of significant arrhythmias in whole cohort (left) and in patients with left ventricular ejection fraction ≥35% (right).

Figure 3: Tracing of the continuous wave-Doppler mitral regurgitation envelope and calculating the average pixel intensity (left panel). The software identifies the numbers of pixels and the pixel intensity and calculates the average pixel intensity in a non-holosystolic (right upper panel) and holosystolic.

Figure 4: Representative figure of the 5 distinct configurations (convergent, divergent, straight, convex or concave) based on 3 measurements (proximal, distal and mid RVOT-PA) using previously applied mathematical modelling.

Figure 5: CCTA revealed intermediate LAD stenosis (Panel A and B). Dynamic CCTA with perfusion defect (Panel C and D).

Figure 6: Short axis (SA) views of the left ventricle in a patient with Takotsubo syndrome with typical apical ballooning. Tracked endo- and epicardial borders are being displayed in apical, midventricular and basal SA views (left panels) with plotted rotation and torsion over a single cardiac cycle (right panel).

References list

1. Reis L, Bispo J, Marmelo B, Oliveira M, Santos R, Domingues K, et al. Gender-correlated differences in a population with hypertrophic cardiomyopathy. A portuguese multicenter study. *Eur Heart J Cardiovasc Imaging* 2017;18(Suppl 3):iii1–5.
2. Liu D, Hu V, Schmidt M, Muentze J, Oder D, Weidemann F, et al. Value of the CHA2DS2-VASc risk score and modified Fabry-specific scores for predicting new-onset or recurrent stroke/TIA in patients with Fabry disease. *Eur Heart J Cardiovasc Imaging* 2017;18(Suppl 3):iii235–7.
3. Stampfli SF, Gotschy A, Kiarostami P, Ozkartal T, Gruner C, Greutmann M et al. Right ventricular morphology and function in left ventricular non-compaction cardiomyopathy. *Eur Heart J Cardiovasc Imaging* 2017;18(Suppl 3):iii235–7.
4. Lie OH, Rootwelt C, Dejgaard LA, Leren IS, Edvardsen T, Haugaa KH. Echocardiography in prediction of life-threatening ventricular arrhythmia in patients with arrhythmogenic cardiomyopathy. *Eur Heart J Cardiovasc Imaging* 2017;18(Suppl 3):iii17–20.
5. Cordeiro F, Ciarka A, Bellmans A, Van Cleemput J, Droogne W, Voros G et al. Global longitudinal strain decreases months before acute humoral but not before acute cellular rejection episode in heart transplant recipients. *Eur Heart J Cardiovasc Imaging* 2017;18(Suppl 3):iii101–2.
6. Tereshina O, Rubanenko A. Absence of contractile reserve associated with a higher risk of further progression of chemotherapy-induced left ventricular dysfunction. *Eur Heart J Cardiovasc Imaging* 2017;18(Suppl 3):iii39–75.
7. Clerc OF, Fuchs TA, Dougoud S, Pazhenkottil AP, Gaemperli O, Kaufmann PA. Direct comparison of SPECT, CACS, CCTA, combined SPECT+CACS and hybrid SPECT/CCTA for long-term prediction of major cardiac events. *Eur Heart J Cardiovasc Imaging* 2017;18(Suppl 3):iii268–303.
8. Galli E, Leclercq C, Hubert A, Smiseth O, Samset E, Hernandez A et al. Role of myocardial constructive work in the identification of responders to CRT. *Eur Heart J Cardiovasc Imaging* 2017;18(Suppl 3):iii268–303.
9. Aalen J, Hisdal J, Storsten P, Remme EW, Larsen CK, Sirnes PA. Pressure-strain loops in the evaluation of left bundle branch block: septal function is aggravated by increased afterload. *Eur Heart J Cardiovasc Imaging* 2017;18(Suppl 3):iii97–100.

10. Klaeboe LG, Lie OH, Dejgaard LA, Haugaa KH, Edvardsen T. Echocardiography can differentiate between athlete's heart and hypertrophic cardiomyopathy genotype positive with mild phenotype. *Eur Heart J Cardiovasc Imaging* 2017;18(Suppl 3):iii13–16.
11. Rodriguez Zanella H, Boccalini F, Secco E, Muraru D, Aruta P, Tenaglia R et al. Left ventricular mechanical dispersion measured with two-dimensional speckle tracking echocardiography predicts severe arrhythmic events in patients with ischemic and non-ischemic cardiomyopathy. *Eur Heart J Cardiovasc Imaging* 2017;18(Suppl 3):iii80–81.
12. Mirea O, Pagourelias ED, Duchenne J, Bogaert J, Thomas JD, Badano LP et al. Vendor specific cut-offs of post-systolic index to identify scarred myocardium. *Eur Heart J Cardiovasc Imaging* 2017;18(Suppl 3):iii17–20.
13. Prevedello F, Nese A, Elnagar B, Genovese D, Surkova E, Cavalli G et al. Right ventricular ejection fraction measured by three-dimensional echocardiography predicts survival better than FAC and TAPSE in patients with various cardiac diseases. *Eur Heart J Cardiovasc Imaging* 2017;18(Suppl 3):iii249–253.
14. Lakatos BK, Tokodi M, Toser Z, Farkas BF, Kovacs PB, Molnar AA et al. Functional shift in right ventricular mechanics following mitral valve repair/replacement: initial results of the PREPARE-MVR study. *Eur Heart J Cardiovasc Imaging* 2017;18(Suppl 3):iii39–75.
15. Palumbo MC, Bandera F, Alfonzetti E, Caiani EG, Guazzi M. 3D echocardiography modeling analysis of right ventricular curvature in left-sided cardiac diseases: implications on pulmonary hypertension severity. *Eur Heart J Cardiovasc Imaging* 2017;18(Suppl 3):iii379–414.
16. Dreyfus J, Ghalem N, Garbarz E, Cimadevilla C, Arangalage D, Verdonk C et al. Isolated tricuspid valve surgery - Early and midterm outcome from French nationwide database and local registry. *Eur Heart J Cardiovasc Imaging* 2017;18(Suppl 3):iii319–353.
17. Fries B, Weidemann F, Hu K, Liu D, Strotmann J, Nordbeck P et al. Impact of myocardial fibrosis on 10-year-outcome in patients undergoing aortic valve replacement. *Eur Heart J Cardiovasc Imaging* 2017;18(Suppl 3):iii238–341.
18. Cacicedo A, Velasco S, Anton A, Onaindia J, Rodriguez I, Oria G et al. Clinical relevance of the pressure recovery phenomenon in asymptomatic severe aortic stenosis. *Eur Heart J Cardiovasc Imaging* 2017;18(Suppl 3):iii182–219.

19. Sanchis Ruiz L, Nijenhuis V, Post MC, Vd Heyden JAS, Swaans MJ. Septal bulge and risk of paravalvular leak after transcatheter aortic valve implantation. *Eur Heart J Cardiovasc Imaging* 2017;18(Suppl 3):iii39–75.
20. Linde L, Carter-Storch R, Christensen NL, Dahl JS, Oevrehus KA, Jensen PS et al. Aortic valve stenosis: correlation between aortic valve calcification by computed tomography and the amount of calcium in the valve. *Eur Heart J Cardiovasc Imaging* 2017;18(Suppl 3):iii238–241.
21. Bech-Hanssen O, Gao SA, Johnsson AÅ, Lagerstrand KM, Polte CL. Evaluation of the integrative algorithm for aortic regurgitation severity by current ASE recommendations using cardiac magnetic resonance as reference method. *Eur Heart J Cardiovasc Imaging* 2017;18(Suppl 3):iii130–166.
22. Gao SA, Polte CL, Lagerstrand K, Johnsson AÅ, Bech-Hanssen O. Evaluation of the integrative algorithm for mitral regurgitation severity by current ASE recommendations using cardiac magnetic resonance as reference method. *Eur Heart J Cardiovasc Imaging* 2017;18(Suppl 3):iii39–75.
23. Kamoen V, El Haddad M, De Buyzere M, De Backer T, Timmermans F. Grading of mitral regurgitation in mitral valve prolapse using the average pixel intensity on continuous wave Doppler. *Eur Heart J Cardiovasc Imaging* 2017;18(Suppl 3):iii39–75.
24. Di Salvo G, Del Gaizo F, Sabatino J, Pergola V, Baldini L, Castaldi B. Exercise induced hypertension in young patients after successful aortic coarctation repair: impact on left ventricular geometry and function. *Eur Heart J Cardiovasc Imaging* 2017;18(Suppl 3):iii106–109.
25. Aguiar Rosa S, Oliveira D, Galrinho A, Branco L, Tiago J, Agapito A et al. Aortic flow and shear stress in bicuspid aortic valve, a multimodality approach. *Eur Heart J Cardiovasc Imaging* 2017;18(Suppl 3):iii106–109.
26. Lesniak-Sobelga AM, Kostkiewicz M, Wisniowska-Smialek S, Holcman K, Hlawaty M, Podolec P. Echocardiographic study of pregnant patients with bicuspid aortic valve. *Eur Heart J Cardiovasc Imaging* 2017;18(Suppl 3):iii106–109.
27. Ivanac Vranesic I, Babu-Narayan SV, Uebing A, Rydman R, Senior R, Swan L et al. Clinical and haemodynamic changes after pregnancy in patients with repaired tetralogy of fallot. *Eur Heart J Cardiovasc Imaging* 2017;18(Suppl 3):iii106–109.
28. Van De Bruaene A, Benson L, Horlick E, Wald R. Relationship between cardiovascular magnetic resonance assessment of native right ventricular outflow tract morphology and

clinical status in adults late after tetralogy of Fallot repair. *Eur Heart J Cardiovasc Imaging* 2017;18(Suppl 3):iii359–361.

29. Hoelscher M, Bonassin FB, Oxenius A, Greutmann M, Lombardi B, Kellenberger C et al. The unnatural course of right ventricular dilatation in patients with severe pulmonary regurgitation after repair of Tetralogy of Fallot. *Eur Heart J Cardiovasc Imaging* 2017;18(Suppl 3):iii106–109.
30. Grotenhuis HB, Friedberg MK, Verpalen IM, Van Den Akker MJE, Dallaire F. Aortic root dilatation and aortic regurgitation in tetralogy of Fallot. *Eur Heart J Cardiovasc Imaging* 2017;18(Suppl 3):iii106–109.
31. Michalak KW, Sobczak-Budlewska K, Szymczyk K, Moll M, Moll JJ, Moll JA. Multimodality assessment of the neoaortic valve regurgitation in adolescents and young adults with transposition of the great arteries after the arterial switch operation. *Eur Heart J Cardiovasc Imaging* 2017;18(Suppl 3):iii359–361.
32. Craft M, Casey C, Bisselou K, Erickson C, Spicer R, Danford D et al. Associations of vector flow derived diastolic indices with traditional indices of left ventricular function in children and young adults. *Eur Heart J Cardiovasc Imaging* 2017;18(Suppl 3):iii130–166.
33. Craft M, Casey C, Bisselou K, Erickson C, Spicer R, Danford D et al. Intraventricular flow characterization by vector flow mapping: do energy distribution curves and wall shear stress provide incremental hemodynamic information in cardiomyopathy? *Eur Heart J Cardiovasc Imaging* 2017;18(Suppl 3):iii359–361.
34. Oleksiak A, Kepka C, Kruk M, Spiewak M, Milosz-Wieczorek B, Marczak M et al. Assessment of myocardial perfusion using dynamic dual source computed tomography in patients with anatomically intermediate coronary artery stenosis. *Eur Heart J Cardiovasc Imaging* 2017;18(Suppl 3):iii76–79.
35. Guglielmo M, Guaricci AI, Andreini D, Mushtaq S, Marconi S, Conti M et al. Left atrial appendage closure guided by 3D printed patient-specific models. *Eur Heart J Cardiovasc Imaging* 2017;18(Suppl 3):iii232–234.
36. Solowjowa N, Meyer A, Hrytsyna Y, Pasic M, Falk V, Knosalla CH. Mitral Valve Reverse Remodeling after Surgical Repair of Acquired Left Ventricular Aneurysms of Posterior versus Anterior Localization Assessed with Multislice Computed Tomography. *Eur Heart J Cardiovasc Imaging* 2017;18(Suppl 3):iii232–234.

37. Guglielmo M, Guaricci AI, Baggiano A, Fazzari F, Andreini D, Calligaris G et al. Stress computed tomographic perfusion improve diagnostic accuracy of coronary computed tomographic angiography in intermediate to high risk patients for coronary artery disease. *Eur Heart J Cardiovasc Imaging* 2017;18(Suppl 3):iii76–79.
38. Holcman K, Kostkiewicz M, Szot W, Wisniowska-Smialek S, Rubis P, Lesniak-Sobelga A et al. Diagnostic value of 99mTc-HMPAO-labeled leukocyte SPECT/CT and transthoracic echocardiography in infective endocarditis. *Eur Heart J Cardiovasc Imaging* 2017;18(Suppl 3):iii76–79.
39. Benetos G, Toutouzas K, Koutagiar I, Skoumas J, Pianou N, Antonopoulos A et al. Familial combined hyperlipidaemia shows increased vascular inflammation compared to heterozygous familial hypercholesterolaemia: insights from an in- vivo imaging study. *Eur Heart J Cardiovasc Imaging* 2017;18(Suppl 3):iii76–79.
40. Eitel I, Stiermaier T, Lange T, Rommel K, Kowallick JT, Lotz J, et al. Cardiac magnetic resonance myocardial feature tracking for optimized prediction of cardiovascular events following myocardial infarction. *Eur Heart J Cardiovasc Imaging* 2017;18(Suppl 3):iii90–93.
41. Lange T, Stiermaier T, Raaz U, Kowallick JT, Lotz J, Hasenfuss G, et al. Temporal course of left ventricular myocardial deformation in Takotsubo syndrome assessed with cardiovascular magnetic resonance myocardial feature tracking. *Eur Heart J Cardiovasc Imaging* 2017;18(Suppl 3):iii182–219.
42. Gonzalez Gomez A, Hinojar R, Esteban A, Fernandez Mendez MA, Carbonell A, Garcia A et al. Incremental value of cardiac deformation analysis in patients severe tricuspid regurgitation and normal right ventricular function: a cardiovascular magnetic resonance imaging study. *Eur Heart J Cardiovasc Imaging* 2017;18(Suppl 3):iii182–219.
43. Hwang JIW, Kim SMOK, Kim SMOK, Park SJI, Park SJI, Kim EUNK et al. Assessment of reverse remodeling predicted by myocardial deformation on tissue tracking in patients with severe aortic stenosis: a cardiac magnetic resonance imaging study. Eur Heart J Cardiovasc Imaging 2017;18(Suppl 3):iii90–93.
44. Gertz RJ, Lange T, Kowallick JT, Backhaus SJ, Unterberg-Buchwald C, Steinmetz M et al. Inter-vendor agreement of left and right ventricular cardiovascular magnetic resonance myocardial feature-tracking. *Eur Heart J Cardiovasc Imaging* 2017;18(Suppl 3):iii182–219.

Figure 1

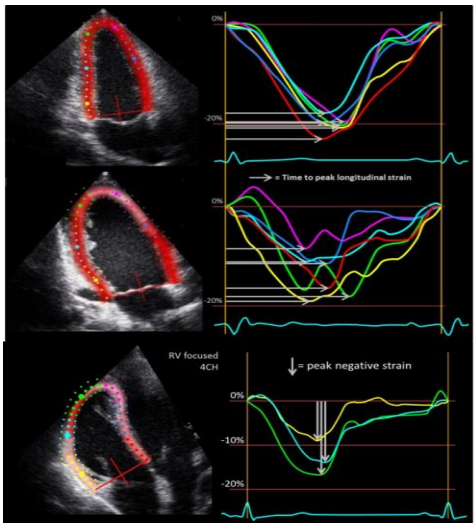
0%
-20%
= Time to peak longitudinal strain
0%
-20%
RV focused
4CH
= peak negative strain
0%
-10%
-20%

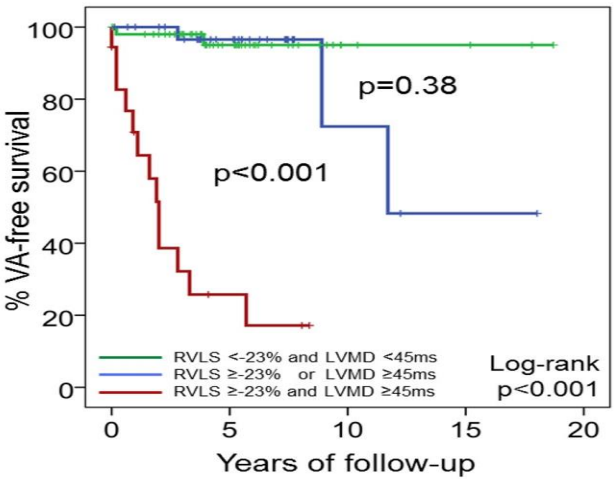
100
80
60
40
20
0
% VA-free survival
p=0.38
p<0.001
RVLS <-23% and LVMD <45ms
RVLS ≥-23% or LVMD ≥45ms
RVLS ≥-23% and LVMD ≥45ms
Log-rank
p<0.001
0
5
10
15
20
Years of follow-up

Figure 2

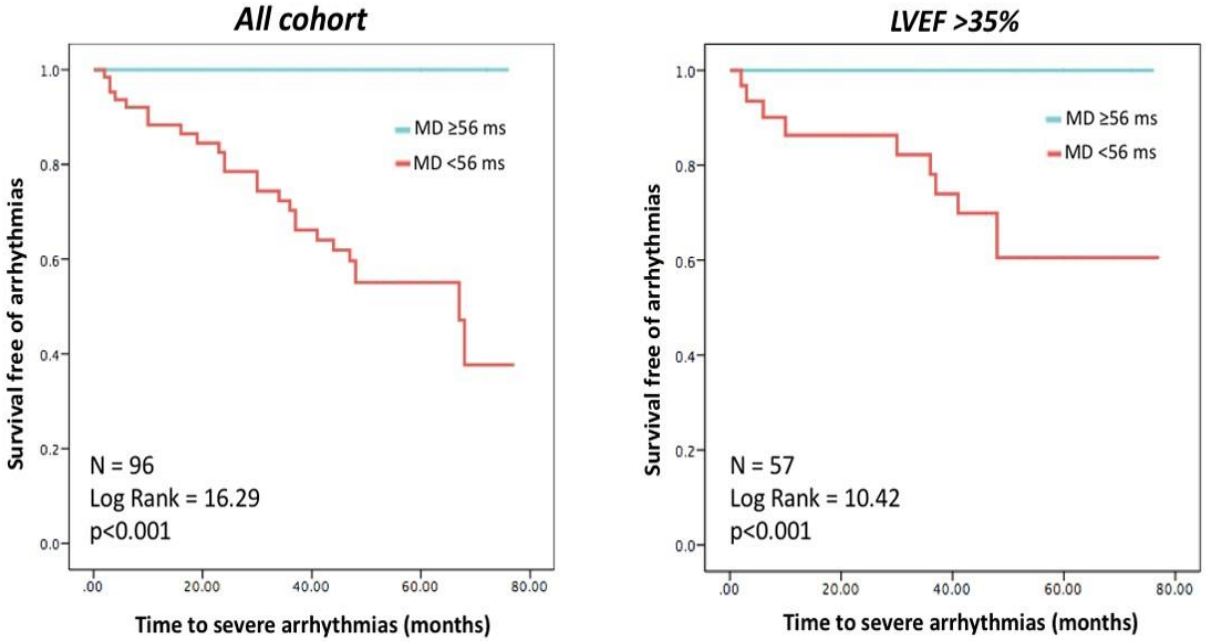
All cohort
Survival free of arrhythmias
1.0
0.8
0.6
0.4
0.2
0.0
MD ≥56 ms
MD <56 ms
N = 96
Log Rank = 16.29
p<0.001
.00
20.00
40.00
60.00
80.00
Time to severe arrhythmias (months)
LVEF >35%
Survival free of arrhythmias
1.0
0.8
0.6
0.4
0.2
0.0
MD ≥56 ms
MD <56 ms
N = 57
Log Rank = 10.42
p<0.001
.00
20.00
40.00
60.00
80.00
Time to severe arrhythmias (months)

Figure 3

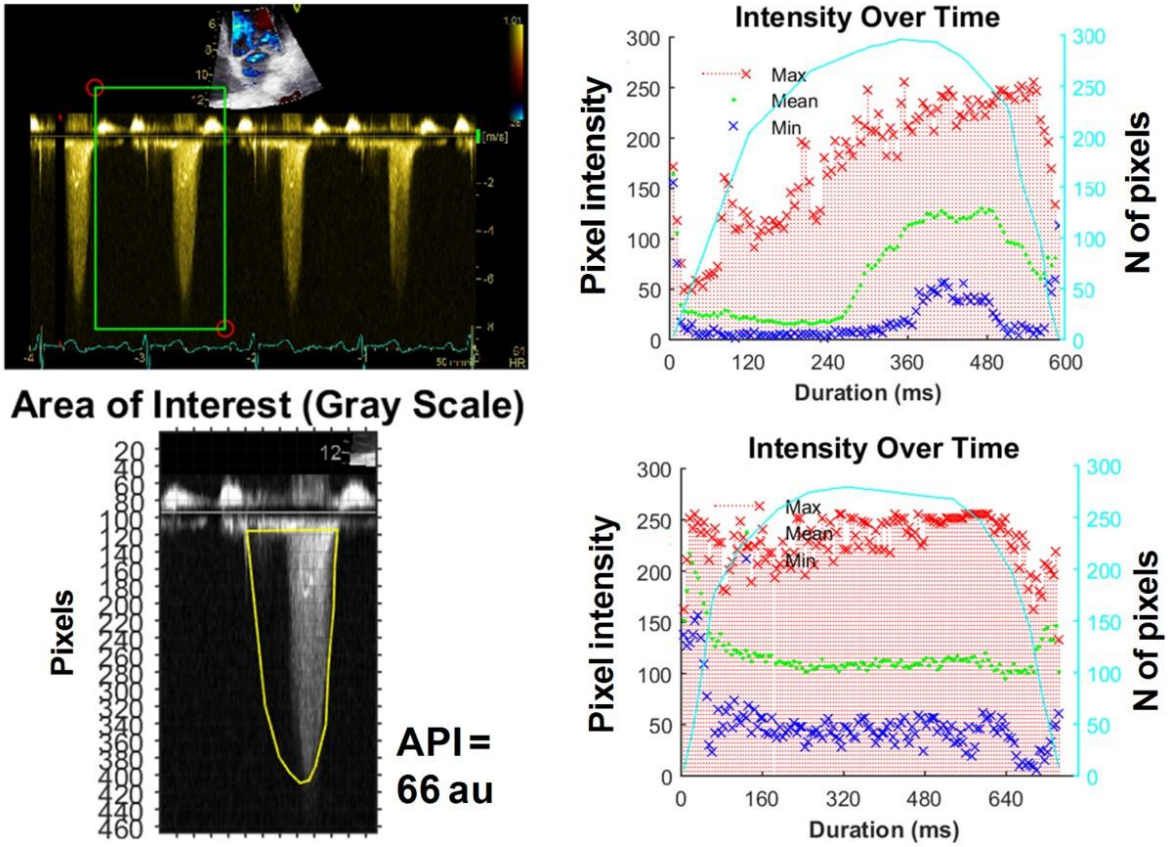
Area of Interest (Gray Scale)
Pixels
API =
66 au
Intensity Over Time
Max
Mean
Min
Pixel intensity
N of pixels
Duration (ms)
Intensity Over Time
Max
Mean
Min
Pixel intensity
N of pixels
Duration (ms)

Figure 4

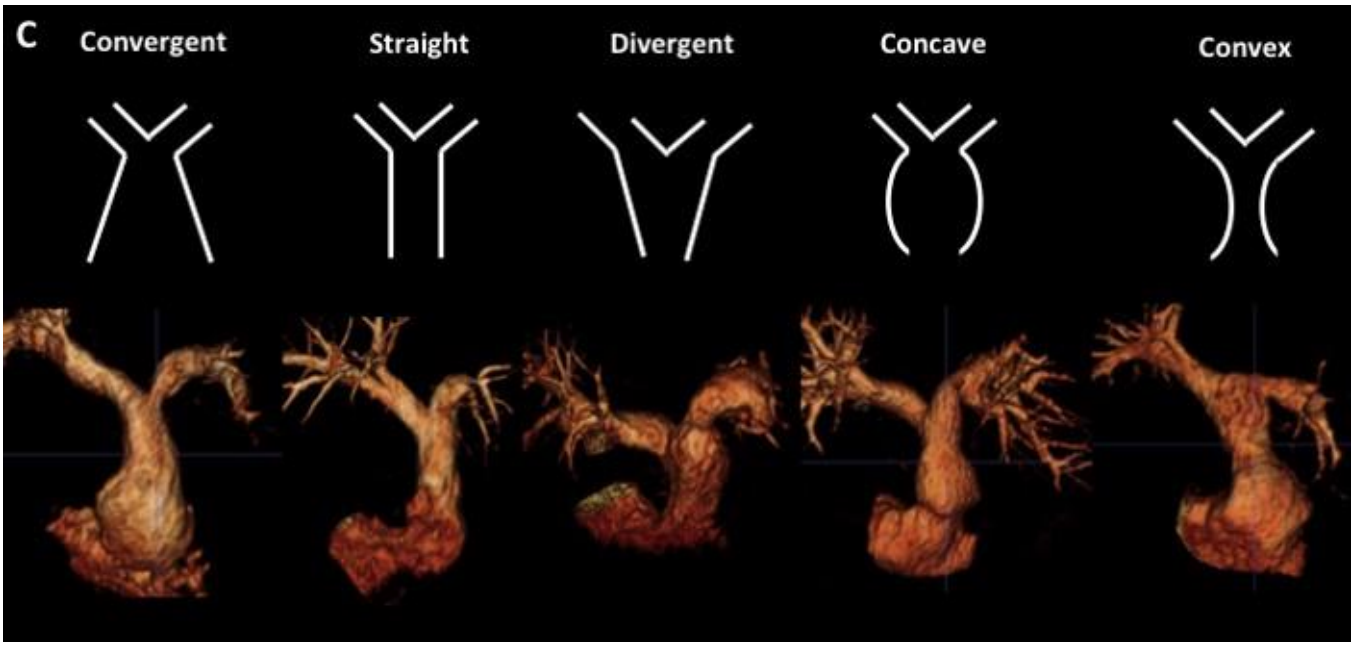

Figure 5

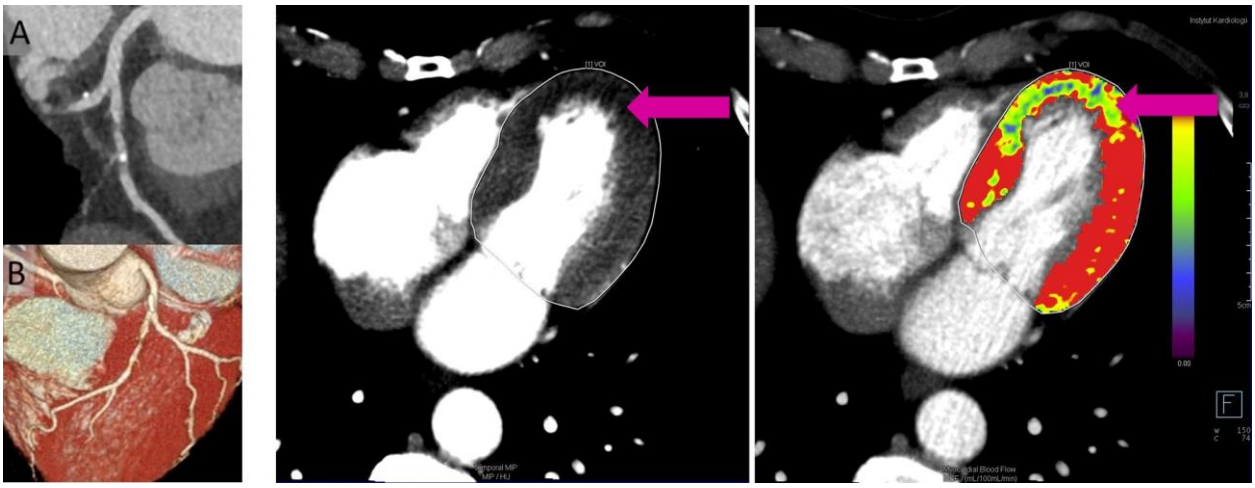

Figure 6

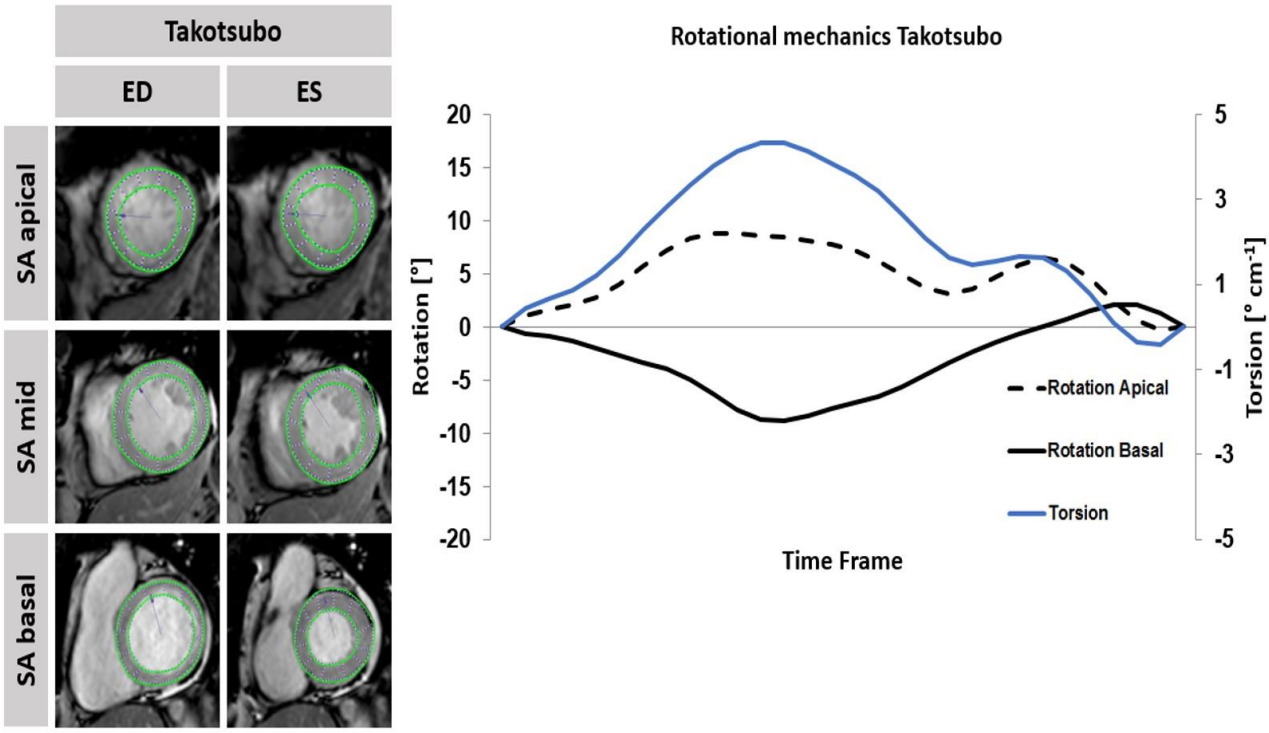
Takotsubo
ED
ES
SA apical
SA mid
SA basal
Rotational mechanics Takotsubo
Rotation [°]
Torsion [° cm-1]
Time Frame
Rotation Apical
Rotation Basal
Torsion
20
15
10
5
0
-5
-10
-15
-20
5
3
1
-1
-3
-5